JOURNAL OF CATALYSIS 116, 144–163 (1989)

Structural Characterization of Cobalt Catalysts on a Silica Support

R. SRINIVASAN,* R. J. DE ANGELIS,* P. J. REUCROFT,* A. G. DHERE,† AND J. BENTLEY‡

*Department of Materials Science and Engineering, University of Kentucky, Lexington, Kentucky 40506; †E. I. Du Pont Company, 4501 North Access Road, Chattanooga, Tennessee 37415; and ‡Metals and Ceramics Division, Oak Ridge National Laboratory, Oak Ridge, Tennessee 37380

Received March 9, 1988; revised October 18, 1988

In situ X-ray diffraction was employed to characterize the structure of several cobalt catalysts on a silica support. The catalysts were reduced in flowing hydrogen at 350°C for about 16 h and X-ray diffraction patterns were collected. After reduction metallic cobalt was found to be present in the hcp and fcc forms in the ratio of 7 : 3 and 17% of the hexagonal close-packed planes were found to be faulted. If surface atoms adjacent to stacking faults are sources of active sites, the density of active sites was estimated to be 4.0×10^{19} per gram of cobalt. © 1989 Academic Press, Inc.

INTRODUCTION

Cobalt is one of the most active catalysts for CO methanation and in the Fischer–Tropsch synthesis, which involves the formation of hydrocarbons by the passage of CO/H_2 mixtures over metallic catalysts at elevated temperatures (*1, 2*). The use of cobalt catalysts is based upon the increased activity and selectivity of hydrocarbon products. This unique behavior has been attributed to its fault structure (*3*). Metal particles of cobalt, supported on ZSM-5, produce bifunctional catalysts that offer shape selectivity due to the channel structure (*4, 5*). A study of the preparation of cobalt catalysts revealed that carbonyl impregnation yielded very small metallic particles with a high degree of dispersion after reduction. The type of impregnation of cobalt onto ZSM-5 has been found to have a considerable effect on the metallic particle size, which is estimated to be at least three times larger for aqueous nitrate impregnation than for carbonyl impregnation (*6*). The selectivity to aromatics was higher with the catalysts prepared by a physical admixture method, while those prepared by impregnation of cobalt nitrate solution yield lower selectivity to aromatics (*7*). Recently it was reported that the cobalt interior to the ZSM-5 is in an irreducible form and the cobalt exterior to the ZSM-5 is in the form of large Co_3O_4 crystallites that are reducible under hydrogen at 350°C to hcp metallic cobalt and CoO. By varying the preparation methods, either of the forms can be obtained (*8*). One of the objectives of this investigation is to identify if the method of preparation has an effect on the formation of the CoO phase.

The addition of a second metal or oxide, usually called a "promoter," to a catalyst is often found to increase the activity and selectivity. Generally this promoter, if added in small amounts, has a significant effect on the activity and the selectivity of the catalysts (*9*). For instance, the addition of thoria as a promoter to cobalt–kieselguhr catalysts resulted in an enhanced yield of C_5^+ hydrocarbons (*10*). A recent investigation on cobalt–thoria–ZSM-5 has revealed that even a small amount of thoria promoter (about 0.4%) causes a remarkable increase in the conversion, shift activity, and C_5^+ selectivity (*7*).

Cobalt catalysts supported on silica support are believed to yield hydrocarbons up to C_{20}^+. The main objective of this paper is to report the results of the structural and mor-

0021-9517/89 $3.00

phological characterization of five cobalt catalysts supported on silica. Since structural defects could be associated with the activity and selectivity of such catalysts, the fault structure is also characterized and discussed.

MATERIALS AND EXPERIMENTAL

The Co/SiO_2 catalysts, used in the present investigation, were supplied by the U.S. Department of Energy, Pittsburgh Energy Technology Center (*11*). The descriptions of these five catalysts are given in Table 1. The support used for impregnating all the cobalt catalysts was Davison 952 silica.

The catalyst CAT-33 was prepared by a carbonyl vapor impregnation technique with 4.1 wt% cobalt on silica. The required amount of silica support was taken in a flask, evacuated, and heated to 360°C for 2 h. It was cooled to room temperature and then again cooled in dry ice. The desired amount of $Co_2(CO)_8$ was mixed with silica and the flask was evacuated again. The mixture was heated at 50°C for about an hour and the temperature was raised to 70°C. The mixture was heated at 70°C overnight in order to decompose the carbonyls and it was cooled in a refrigerator overnight prior to being exposed to the atmosphere (*12*). The catalyst CAT-153 containing 6.0 wt% cobalt was made by aqueous nitrate impregnation of cobalt nitrate with silica. Aqueous nitrate impregnation involves dissolving the desired amount of metal nitrate in water and impregnating the solution on to the support until incipient wetness is reached, and then drying the catalyst at about 110°C. The catalyst CAT-171A was made by physically admixing 14.4 wt% precipitated cobalt (as oxide) with silica. The catalyst CAT-65 was prepared from a physical admixture of 14.2 wt% precipitated cobalt (as oxide) and 0.8 wt% Cu (as oxide) with silica. The catalyst CAT-18A was obtained by the same admixture technique from 4.8 wt% cobalt (as oxide) and 0.8% wt% Th (as thoria) with silica. In the physically admixed preparation, cobalt oxide was initially made as a precipitate by adding 10 wt% sodium carbonate solution at 70°C to a second solution also at 70°C, containing the desired amount of cobalt nitrate until a final pH of 7 was reached. In the case of promoters, cobalt nitrate and thorium nitrate or copper nitrate solutions were coprecipitated by the addition of sodium carbonate solution. The resulting precipitate was filtered, washed with water several times to reduce the content of sodium to less than 0.1 wt%, and dried at 110°C. The dried metal oxide was physically mixed with the silica support (*12*).

TABLE 1

Specifications of the Cobalt Catalysts under Investigation

Reference Id.	Method of preparation	Wt% cobalt	Wt% promoter
CAT-33	Carbonyl vapor impregnation	4.1	—
CAT-153	Aqueous nitrate impregnation	6.0	—
CAT-171A	Physical admixture	14.4	—
CAT-65	Physical admixture	14.2	0.8% Cu
CAT-18A	Physical admixture	4.8	0.8% ThO_2

The catalyst powders were ground and pressed into a disk of 18 mm in diameter and 2 mm thick in an aluminum holder. This was mounted into an *in situ* high-temperature X-ray diffraction camera, installed on a Picker X-ray diffractometer. All treatments to a specimen were performed *in situ*, ensuring that the same volume of the sample was observed during the experiment. A nickel target X-ray tube operating at 35 kV and 8 mA was used as the source of radiation, with a single bent graphite monochromator in the diffracted beam path. All the X-ray diffraction data are replotted in terms of Cu$K\alpha$ radiation for the purpose of comparison to other data and are presented under Results in terms of Cu$K\alpha$ radiation.

The removal of moisture present on the surface of the catalysts was ensured by heating the sample at 150°C for about an hour in a helium atmosphere. The camera was evacuated to less than 10^{-3} Torr at 150°C. These two steps were taken in order to ensure the total absence of water vapor

on the catalyst surface, because the removal of water vapor formed during the preparation and reduction processes favors the formation of small metallic particles. The temperature was then lowered to 50°C and hydrogen gas at a flow rate of 60 cc/min was introduced into the camera. The temperature was raised to 350°C at a rate of 2°C/min and the catalysts were reduced at this temperature in hydrogen for 16 h. Then the hydrogen was replaced by helium and the temperature was reduced to ambient and the X-ray diffraction patterns from the reduced samples were collected *in situ*. Prior to removing a specimen from the camera, it was passivated at room temperature for 24 h with a 2.0% oxygen–nitrogen mixture. The reduction temperature of 350°C was selected in order to avoid the transformation of hcp cobalt to fcc cobalt at about 415°C. The sequence of treatments is presented in Fig. 1.

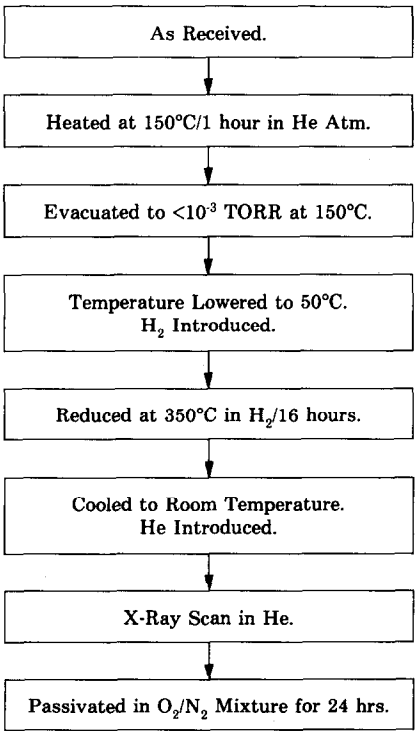

FIG. 1. Flow diagram of successive treatments given to cobalt catalysts.

TEM samples were prepared by suspending the passivated catalyst powders in absolute alcohol. While the suspension was constantly agitated ultrasonically, a drop of this suspended solution was carefully placed on a carbon-coated Formvar film predeposited on a copper grid. These samples were examined in a Philips EM400T microscope equipped with a field emission gun, a 6585 STEM unit, and an EDAX 9100/70 system at Oak Ridge National Laboratory. The microscope was operated at 100 kV.

RESULTS

1. X-Ray Diffraction Studies

The X-ray diffraction patterns collected from all the as-received catalysts prior to reduction exhibited cubic Co_3O_4 phase. However, CAT-33 showed no significant cobalt or cobalt oxide peaks prior to and even after reduction (see Fig. 2). This may be due to the existence of very small particles (<2 nm) in the carbonyl-impregnated sample, which caused extensive broadening of cobalt peaks. The X-ray diffraction pattern of the reduced sample is shown in Fig. 2, with the calculated positions of all cobalt peaks indicated by arrows.

The X-ray diffraction patterns obtained from the catalyst CAT-153 after reduction are presented in Figs. 3a and 3b. These diffraction patterns consisted of a sharp, intense hcp Co(002) peak, a well-broadened Co(101) peak, an overlapped Co(100), and CoO(200) peaks in addition to a broad CoO(111) peak. The sharp intense peak of Co(110) is also shown in Fig. 3b.

The X-ray diffraction patterns collected from the catalyst CAT-171A after reduction are depicted in Figs. 4a and 4b. These diffraction patterns consisted of hcp Co(002), Co(101), Co(110), an overlapped Co(100), and CoO(200) and CoO(111) profiles. The expected position of CoO(200) is indicated by the arrow. This diffraction pattern was also found to consist of a diffuse and very broad (200) peak from fcc cobalt at 2θ =

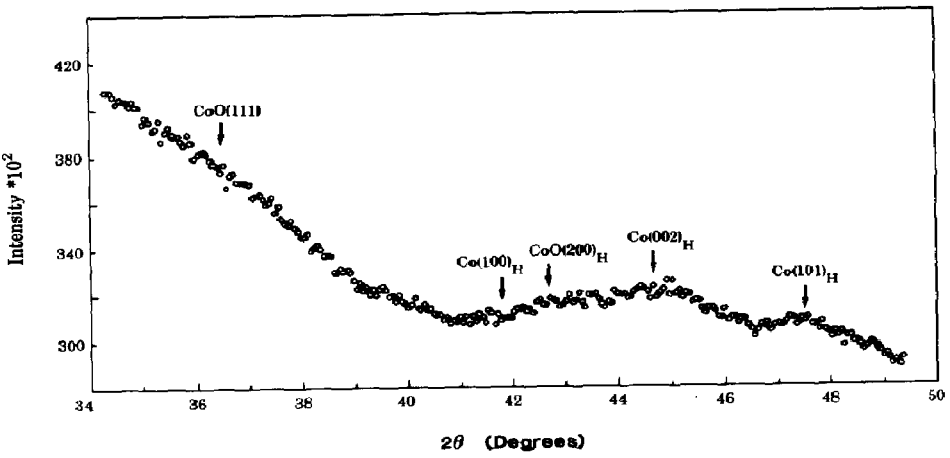

FIG. 2. XRD pattern from the reduced catalyst CAT-33 with 4.1 wt% cobalt prepared by carbonyl impregnation (Cu$K\alpha$ radiation). The arrows indicate the positions of cobalt peaks.

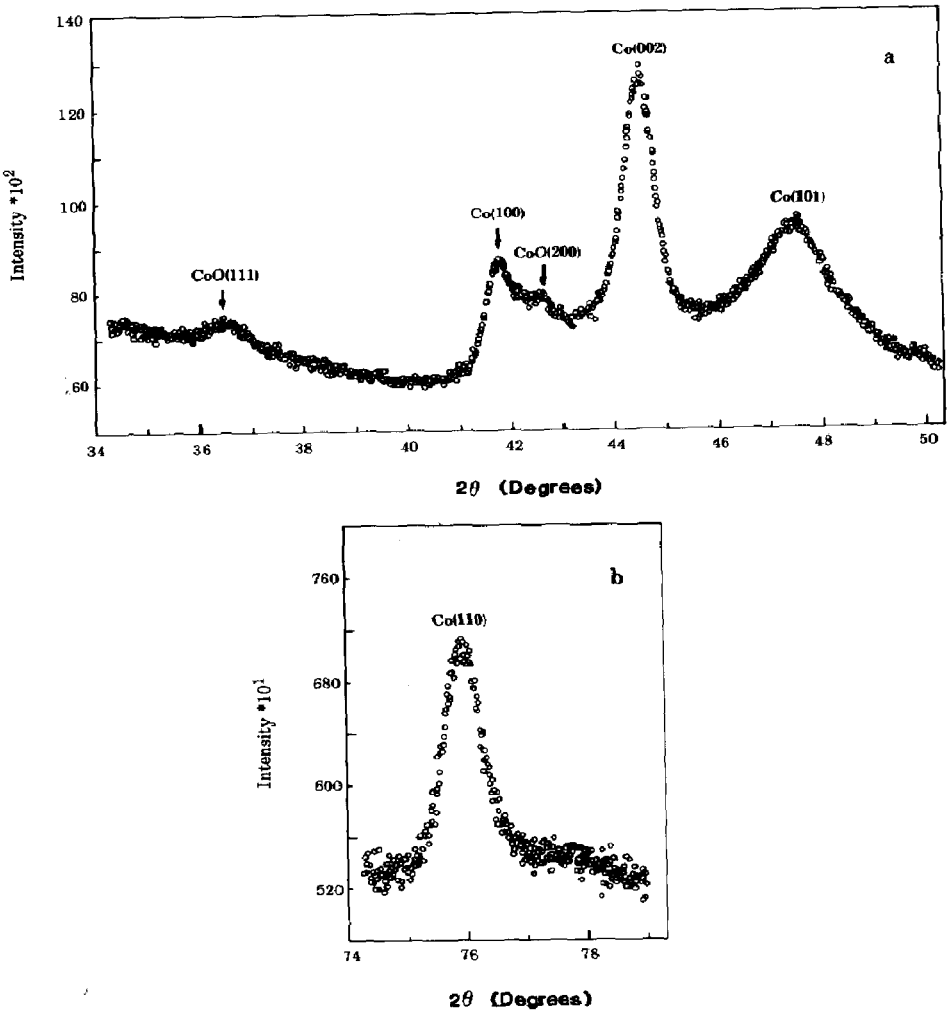

FIG. 3. XRD patterns from the reduced catalyst CAT-153 with 6.0 wt% cobalt, prepared by aqueous cobalt nitrate impregnation (Cu$K\alpha$ radiation). (a) $2\theta = 34°–52°$ and (b) $2\theta = 74°–79°$.

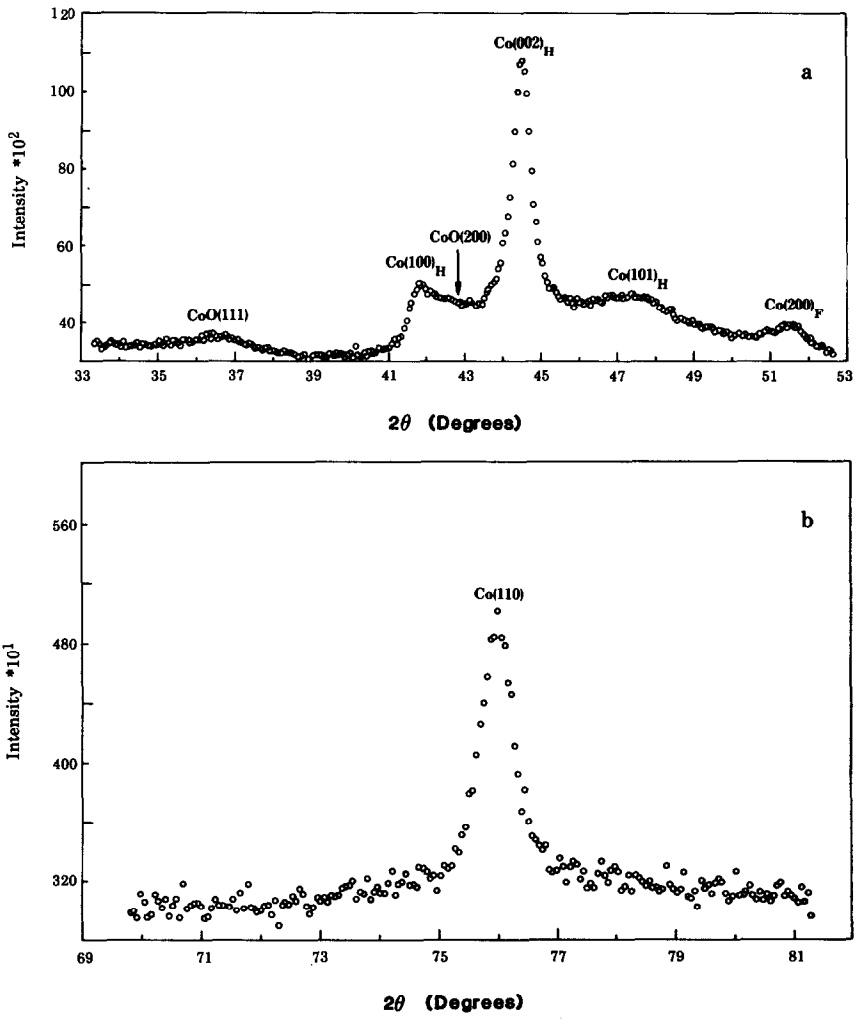

FIG. 4. XRD patterns from the reduced catalyst CAT-171A, with 14 wt% cobalt by physical admixture technique (Cu$K\alpha$ radiation). (a) 2θ = 33°–53° and (b) 2θ = 69°–81°.

51.6° (Cu$K\alpha$ radiation). An attempt to collect fcc cobalt peaks at higher angles failed to yield reliable and clear results, owing to the extensive overlapping of fcc and hcp cobalt peaks. The only independent fcc cobalt peak is (200), which occurs at 2θ = 51.6° as can be seen in Fig. 4a.

The X-ray diffraction patterns from the catalyst CAT-65 after reduction are shown in Figs. 5a and 5b, which are similar to those of CAT-171A. The absence of a detectable CoO phase can be noted in this pattern.

The X-ray diffraction patterns collected from the catalyst CAT-18A after reduction are presented in Figs. 6a and 6b, in which all the significant peaks of metallic cobalt can be seen, while the CoO profile is quite obscure. The respective integrated intensity data of all the peaks identified in these five catalysts are presented in Table 2. In the cases where the peaks overlapped, the best estimates of the integrated intensities were made by constructing the shape of the individual profiles. The integrated intensity of the hcp Co(101) profile for CAT-153 was

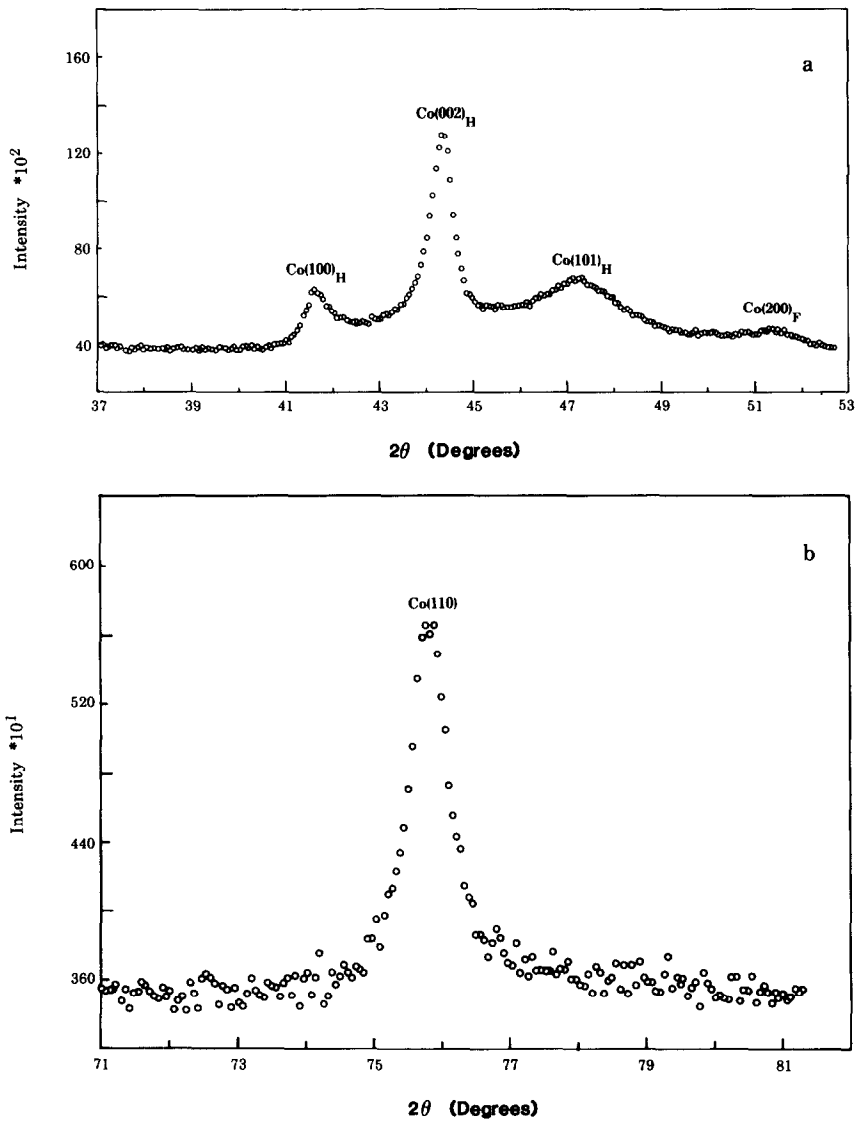

FIG. 5. XRD patterns from the reduced catalyst CAT-65, with 14.2 wt% cobalt +0.8 wt% Cu prepared by physical admixture technique (Cu$K\alpha$ radiation). (a) 2θ = 37°–53° and (b) 2θ = 71°–81°.

anomalously large for reasons unknown (Fig. 3a).

2. *Particle Size Analysis*

Particle sizes were calculated using both the Scherrer equation and a Fourier single profile analysis (*13*) for all the catalysts. However, particle size analysis could not be made for the catalyst, CAT-33, as no well-defined peaks appeared in the X-ray diffraction pattern (Fig. 2).

Cat-153. The average particle size of the hcp Co(101) peak measured by the Scherrer equation was found to be 5 nm. The particle size distribution calculated from the shape of this profile, using the single profile analysis technique (*13*), yielded a particle size of 4 nm (Fig. 7a). The particle sizes calculated from the CoO(111) and Co(002) profiles by

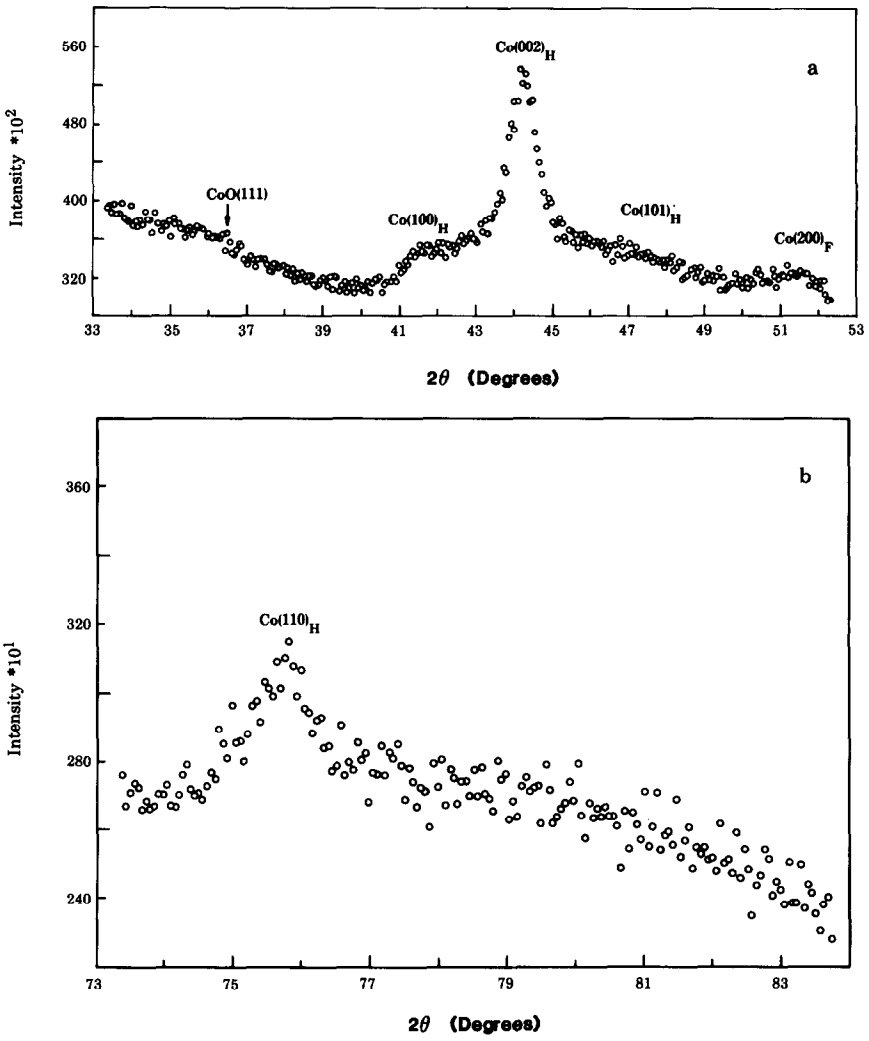

FIG. 6. XRD patterns from the reduced catalyst CAT-18A, with 4.8% cobalt +0.8 wt% ThO_2 by physical admixture technique (Cu$K\alpha$ radiation). (a) 2θ = 33°–53° and (b) 2θ = 73°–84°.

TABLE 2

Integrated Intensities of Observed X-Ray Profiles

Reference Id.	CoO(111)	Integrated intensity (arbitrary units)					
		CoO(200)	$Co(100)_{hcp}$	$Co(002)_{hcp}$	$Co(101)_{hcp}$	$Co(110)_{hcp}$	$Co(200)_{fcc}$
CAT-33	—[a]	—	—	—	—	—	—
CAT-153	1.75	0.73	5.0	10.25	17.1	4.55	Δ
CAT-171A	1.5	0.50	6.25	19.60	8.65	7.12	3.35
CAT-65	Δ[b]	A[c]	5.9	29.5	10.3	6.86	3.2
CAT-18A	—	—	2.4	8.50	—	3.10	1.30

[a] —, could not be determined.
[b] Δ, not available.
[c] A, absent.

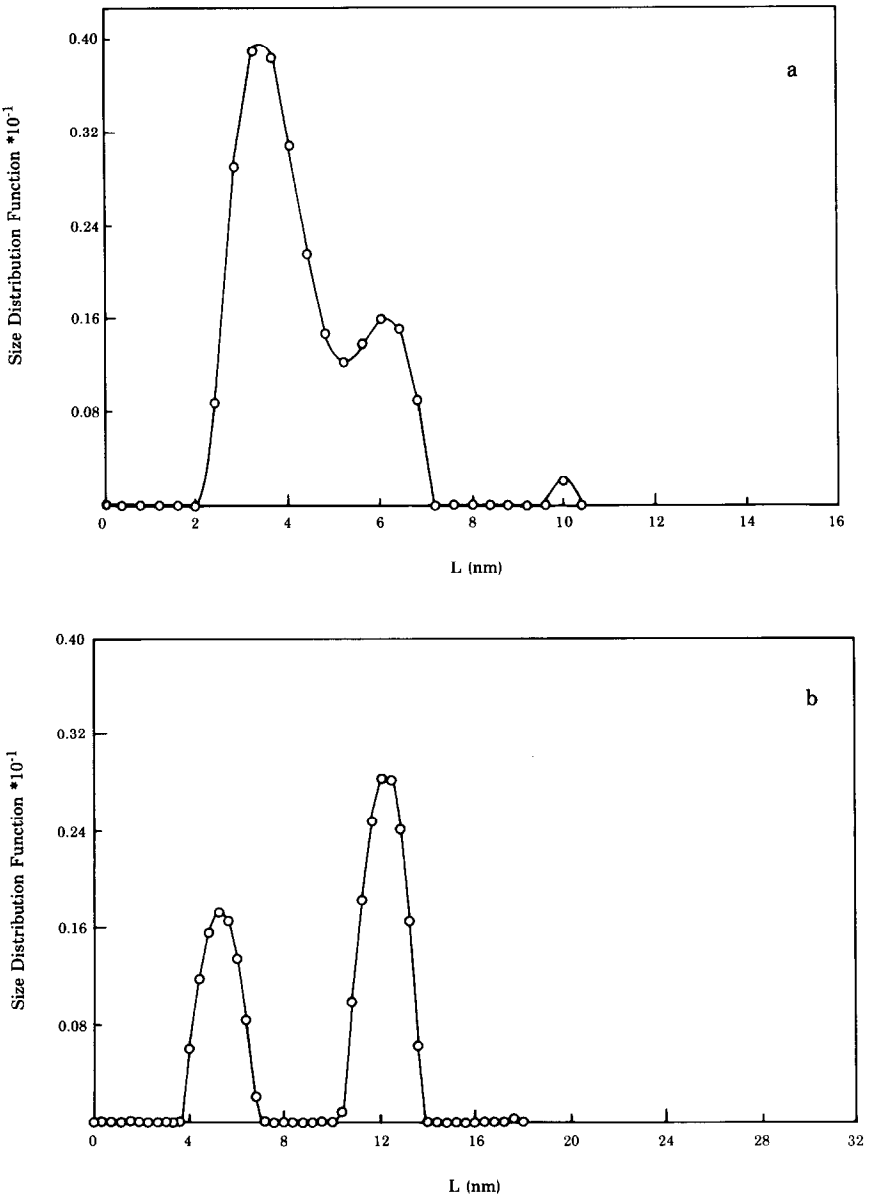

FIG. 7. Particle size distribution function vs particle size of CAT-153 for (a) Co(101) and (b) Co(110).

the Scherrer equation were 10 and 13 nm, respectively. The Scherrer equation for the hcp Co(110) profile yielded a value of 14 nm and the particle size distribution for this profile was observed to be bimodal (Fig. 7b) with two modes at 5 and 12 nm.

CAT-171A. The particle sizes of the CoO(111) and Co(002) profiles determined by the Scherrer equation were 7 and 16 nm, respectively. The particle size of the Co(101) peak calculated using the Scherrer equation was 4 nm and the single profile analysis of this peak yielded a particle size of 4 nm (Fig. 8a). For the Co(110) profile a bimodal distribution was obtained with modes at 12 and 17 nm, as shown in Fig. 8b.

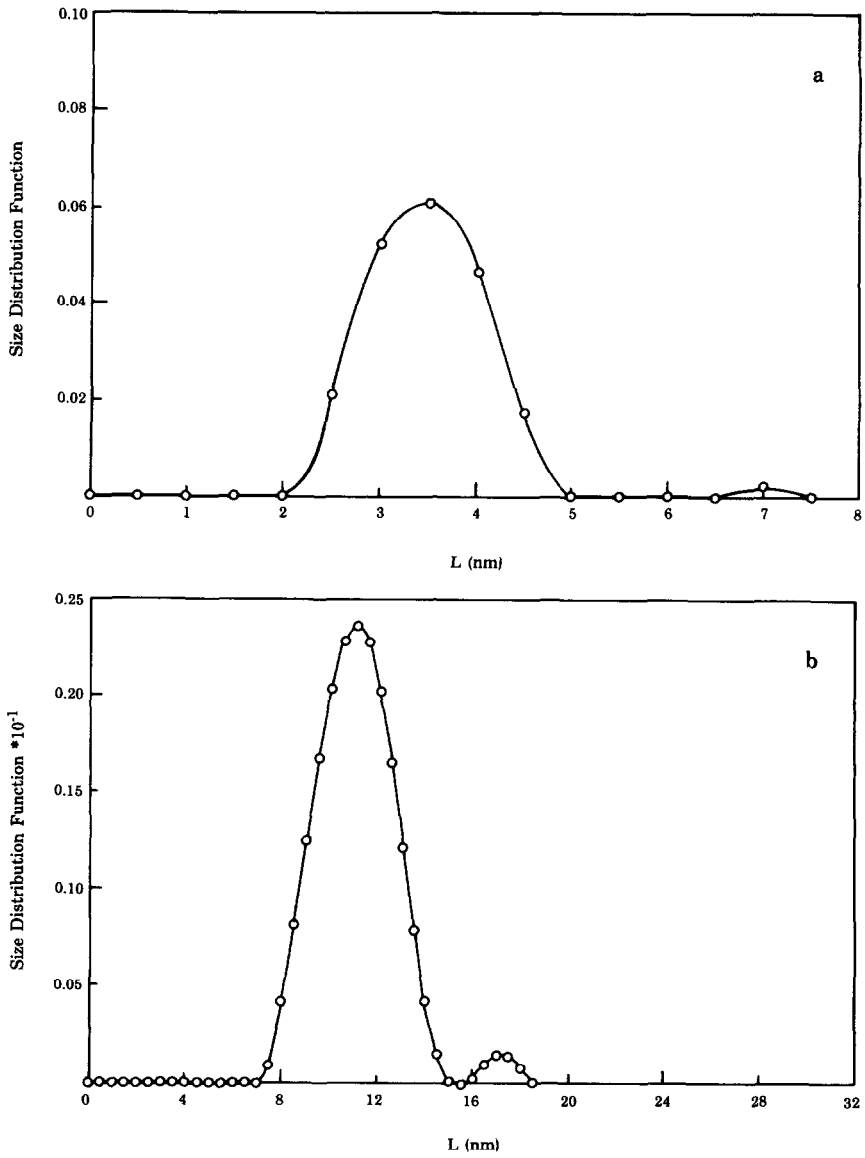

FIG. 8. Particle size distribution function vs particle size of CAT-171A for (a) Co(101), (b) Co(110), and (c) $Co(200)_{fcc}$.

The Fourier single profile analysis for the fcc Co(200) profile showed a bimodal distribution with modes at 6 and 11 nm (Fig. 8c).

CAT-65. The particle size of the hcp Co(002) profile estimated using the Scherrer equation was found to be 14 nm. For the Co(101) profile, the Scherrer equation and the single profile analysis yielded values of 4 and 5 nm, respectively. The Scherrer equation gave a value of 2 nm for the Co(110) profile, while the single profile analysis for the same peak showed bimodal distributions with modes at 5 and 12 nm, the average of which was about 10 nm. The execution of the single profile analysis on the fcc Co(200) profile yielded a particle

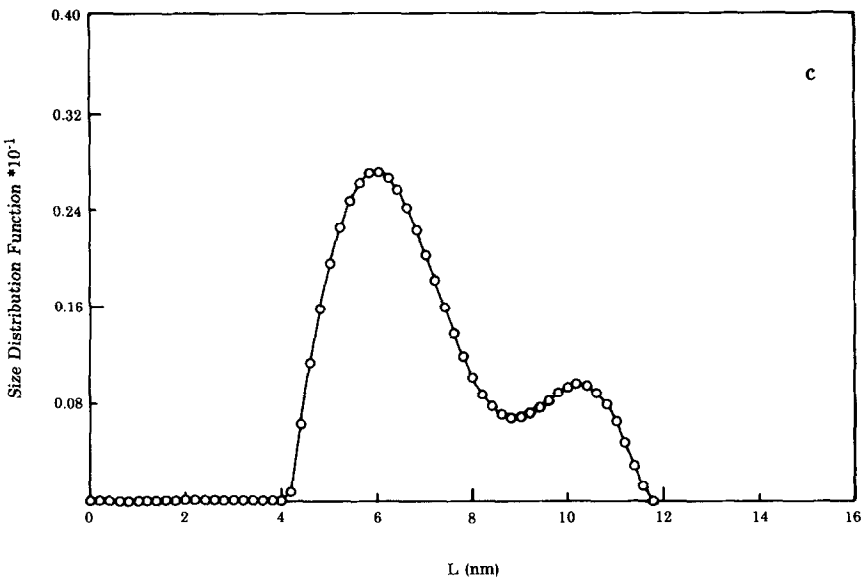

FIG. 8—*Continued.*

size estimate of about 4 nm. The particle size distribution functions are shown in Figs. 9a–9c.

CAT-18A. The particle size of the Co(002) profile from the Scherrer equation was found to be about 12 nm. As the Co(101) profile was very broad and diffuse, particle size analysis could not be carried out. However, the scattered data for the Co(110) profile were smoothened and the Scherrer equation yielded a particle size of 6 nm, while the single profile analysis gave a value of 5 nm (Fig. 10a). The single profile analysis for the fcc Co(200) profile gave a value of 10 nm (Fig. 10b).

The complete particle size measurement data for all the observed peaks are tabulated in Table 3.

3. *Determination of Growth Fault Probability*

The growth fault probability, β, was estimated from the particle sizes of the Co(110) and Co(101) profiles, using the faulting relationship developed by Warren (*14*). These results yielded a β value of about 0.16–0.18, and the inverse of β is the average number of planes between the faults, which was about 5–6.

4. *Calculation of Percentage of fcc Phase*

The presence of the fcc phase was identified in three of the reduced catalysts. The percentage of the fcc phase was calculated from the integrated intensities of the $(200)_{fcc}$ and $(100)_{hcp}$ profiles using the two-phase relationship. These calculations indicated the presence of about 30% fcc phase in CAT-65, CAT-18A, and CAT-171A.

5. *Determination of Number of Active Sites*

The number of surface atoms per gram of cobalt was calculated from the following relationship, assuming the cobalt particles to be spherical in shape,

$$N = \frac{2\pi \hat{r} n}{a_0 \rho_{Co} V_p}, \qquad (1)$$

where N is the surface atoms per gram of cobalt; $\hat{r}$, the average radius of the particle (nm); a_0, the length of the a axis (nm); ρ_{Co},

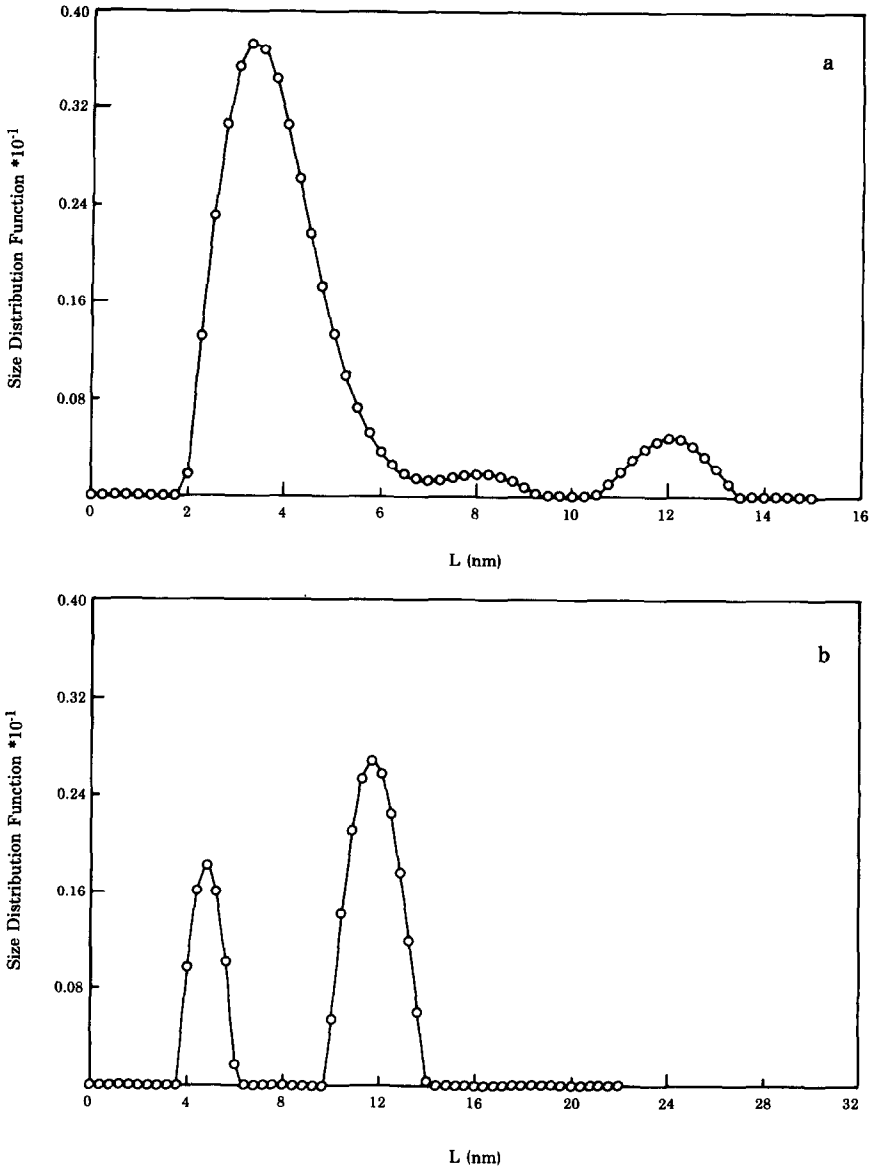

FIG. 9. Particle size distribution function vs particle size of CAT-65 for (a) Co(101), (b) Co(110), and (c) $Co(200)_{fcc}$.

the density of cobalt (g/cc); V_p, the volume of the spherical particle (cm^3); n, the number of planes per particle. The value of n was determined from the relationship

$$n = \frac{2R\beta}{c_0/2}, \qquad (2)$$

where R is the radius of the particle; β, the fault probability; c_0, the length of the c axis. Assuming the average cobalt particle size of 15 nm, which is comparable to the value obtained from the X-ray data, the number of planes n was calculated. Substitution of n and other constants in Eq. (1) yielded N, the number of surface atoms per gram of

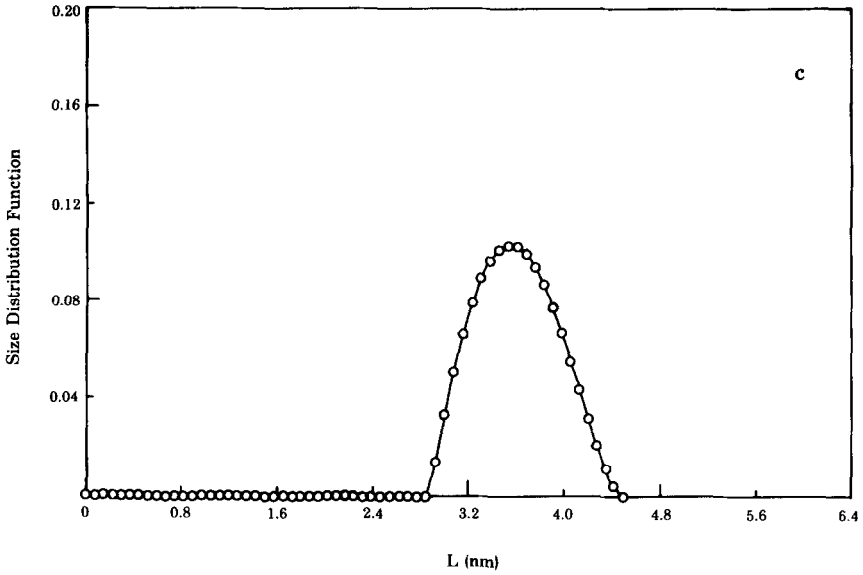

FIG. 9—*Continued.*

cobalt. N was found to be 2.5×10^{20}. This value when multiplied by the fault probability β yielded a value of 4.0×10^{19}, the number of active sites per gram of cobalt, assuming that the active sites are associated with the faults.

6. *TEM Results*

Bright-field images from the catalyst samples prepared by physical admixture technique are shown in Figs. 11–15. Cobalt particles are seen as dark areas on the lighter background of the silica support. The micrograph of CAT-171A in Fig. 11 indicates the average size of the cobalt particle to be about 36 nm. The micrograph of CAT-65 is shown in Fig. 12, wherein the average cobalt particle size is about 34 nm. Stacking faults were observed in several cobalt particles in these figures and the distance between the stacking faults was about 3 nm. The stacking fault spacing was in good agreement with the value calculated from the X-ray data.

DISCUSSION

The carbonyl impregnated catalyst CAT-33 failed to exhibit any metallic cobalt peaks after reduction at 350°C. This was due to the fact that carbonyl-impregnated cobalt catalysts are known to yield a high degree of dispersion of metallic particles after reduction treatment (*6*), which cause the extensive broadening of X-ray profiles.

The catalyst CAT-153, prepared by an aqueous impregnation technique with a cobalt loading of 6.0 wt%, indicated the presence of hcp metallic cobalt and also the CoO phase. CAT-171A, which was prepared by the precipitation technique and contained 14.4 wt% cobalt, showed an X-ray diffraction pattern, which was similar to that of CAT-153 with an obscure CoO phase. The fault probability was also the same for both. The particle sizes determined for all the profiles from these two samples are more or less the same. Neither of these catalysts contained promoters. It appears that a lower percentage of cobalt loading prepared by the aqueous impregnation technique may yield similar results in the activity studies, as a higher percentage of cobalt loading prepared by the precipitation technique.

The catalysts CAT-171A and CAT-65 were both prepared by the physical admix-

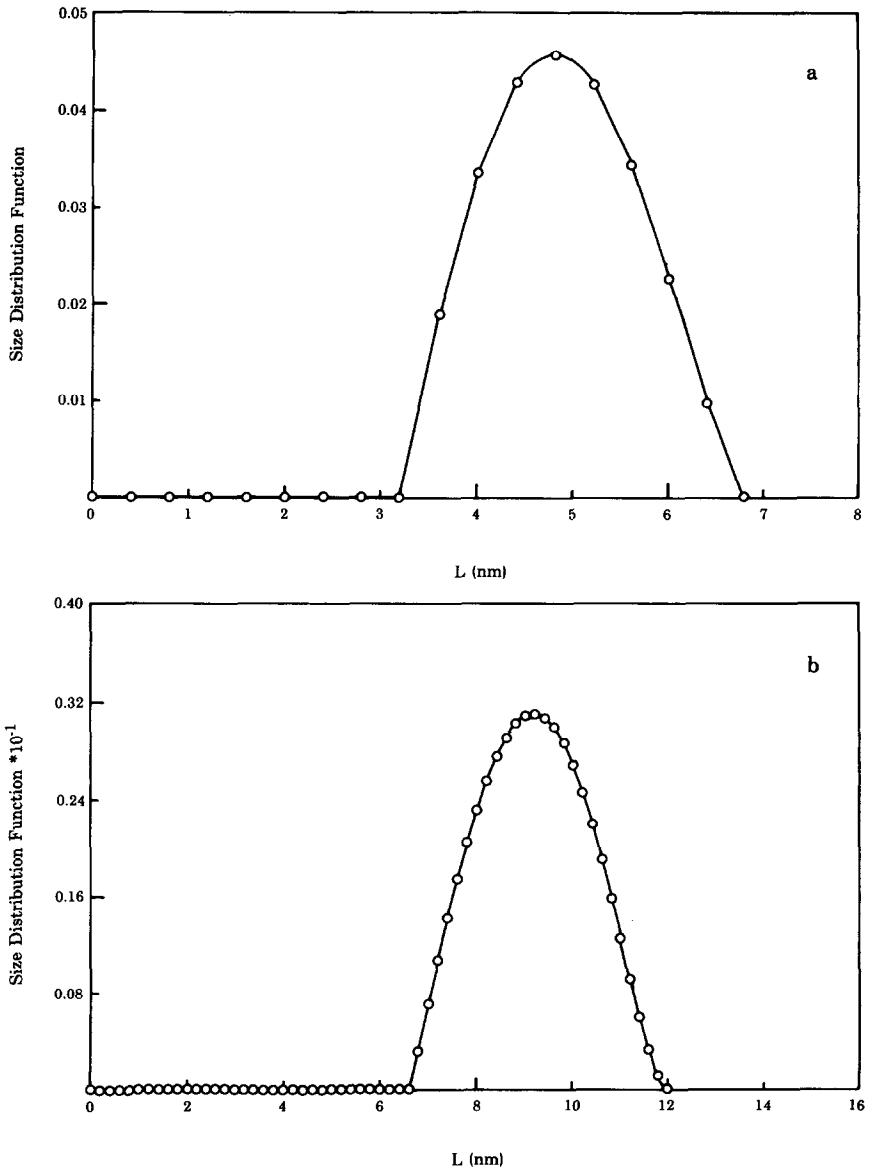

FIG. 10. Particle size distribution function vs particle size of CAT-18A for (a) Co(110) and (b) $Co(200)_{fcc}$.

ture method. While the former contained 14.4 wt% cobalt without any promoters, the latter had about the same cobalt loading with 0.8% wt% Cu as a promoter. While a broad and diffuse CoO(200) peak is hardly seen in CAT-171A, this phase is practically absent in CAT-65 (compare Figs. 4a and 5a). All cobalt oxide in CAT-65 appears to have been fully reduced to metallic cobalt. The absence of CoO phase in all the catalysts prepared by the precipitation technique indicates that this technique produces catalysts in which CoO is completely reduced to metallic cobalt after the reduction treatment. The particle size and fault probability for both these catalysts are comparable.

The catalyst CAT-18A, which was pre-

TABLE 3

Particle Size Measurement Data (nm)

Sample Id.	CoO(111) Scherrer	Co(002) Scherrer	Co(101)		Co(110)			
			Scherrer	PSD	Scherrer	PSD		
						M1	M2	Average
CAT-33	—[a]	—	—	—	—	—	—	—
CAT-153	10	13	5	4	14	6	13	10
CAT-171A	7	16	5	4	15	11	17	12
CAT-65	Δ[b]	14	4	5	16	5	12	10
CAT-18A	—	12	—	—	6	5	NA[c]	5

[a] —, could not be determined.
[b] Δ, not available.
[c] NA, not applicable.

pared by the precipitation technique, contained 4.8 wt% cobalt with 0.8 wt% ThO_2 as the promoter. ThO_2 is known to increase the selectivity of C_5^+ and higher hydrocarbon products (*15*). The absence of CoO phase and the presence of fcc cobalt in the X-ray diffraction of this catalyst are noteworthy.

Selective broadening due to faults in the hcp Co(101) reflection was observed in all the samples studied in the present investigation. The particle sizes measured from the (101) reflections were always smaller than those measured for other peaks of the same sample (see Table 3). This behavior of selective broadening is related to the existence of stacking faults in the hcp cobalt (*14*). The average particle size estimates for this fault-affected profile from the Scherrer equation and the Fourier single profile analysis for all catalysts are in the neighborhood of 4.5 nm. Because the faulting is heavy, the average distance between the faults can conveniently be assumed to be the particle size of the Co(101) profile, which is affected by faulting. Assuming the presence of only growth faults caused by heat treatments, the probability of faulting for all the samples is found to be in the neighborhood of 0.16. This indicates that every sixth hexagonal close-packed plane is faulted. Earlier observation on Co/ZSM-5 indicated that there was an average of 12 planes between the faults (*16*). Thus it is clear that in Co/SiO_2 the density of faulting is twice as high as that in Co/ZSM-5. An increase in faulting may result in an enhanced activity and selectivity of the cobalt catalysts on silica support. In the present investigation, the number of surface atoms per gram of cobalt is found to be 2.5×10^{20}, of which about 4.0×10^{19} would be the number of active sites. However, only 4×10^{17} active sites per gram of cobalt were estimated for Co/ZSM-5 (*17*). Thus the increase in the number of faults may play an important role in the enhancement of activity and selectivity of the Co/SiO_2 catalysts. The results thus indicate that increased stacking fault density may favor the formation of products of higher molecular weight and inhibit the formation of products of lower molecular weight. This is consistent with recent results (*18*) on the effect of the allotropic transformation of cobalt on the rate of methanation of CO_2. In this study, it was found that the rate of methanation produced by the fcc (high temperature) form of cobalt was lower than that produced by the hcp (low temperature) form.

Stacking faults in cobalt reduce the diffracting particle size as can be seen in the

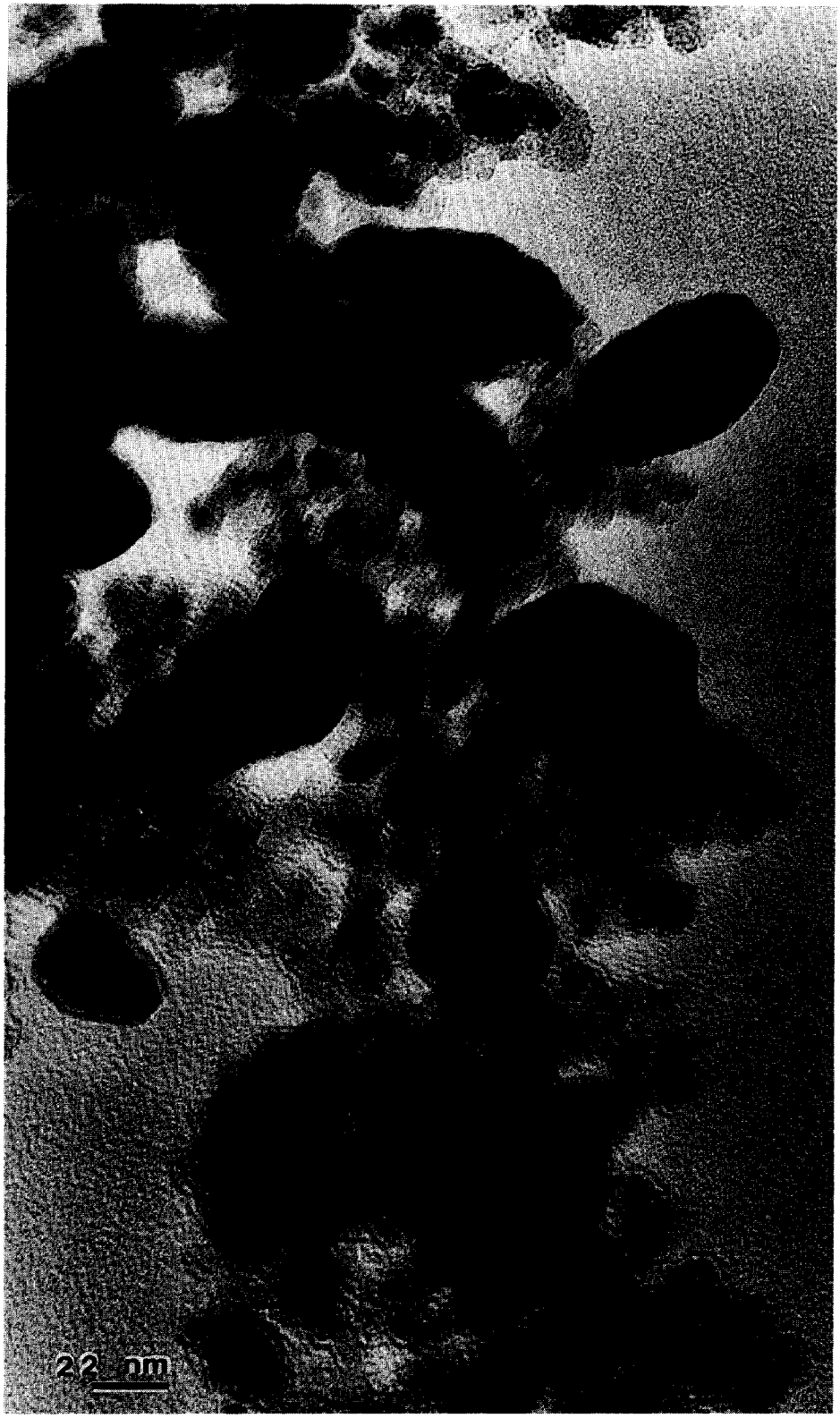

FIG. 11. The bright-field micrograph of CAT-171A, prepared by physical admixture technique with 14.4 wt% cobalt.

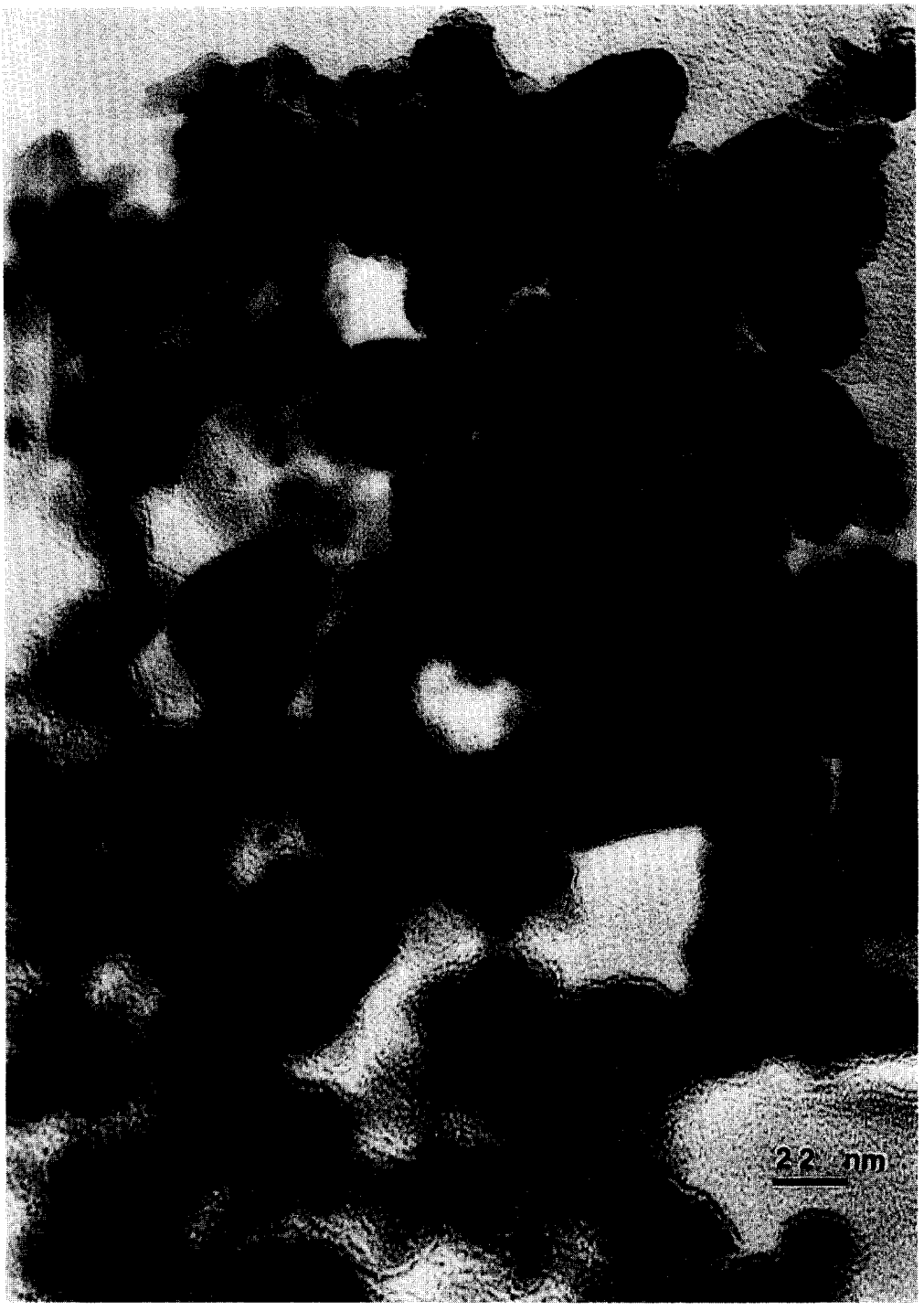

FIG. 12. The bright-field micrograph of CAT-65, prepared by physical admixture technique with 14.2 wt% cobalt and 0.8 wt% Cu.

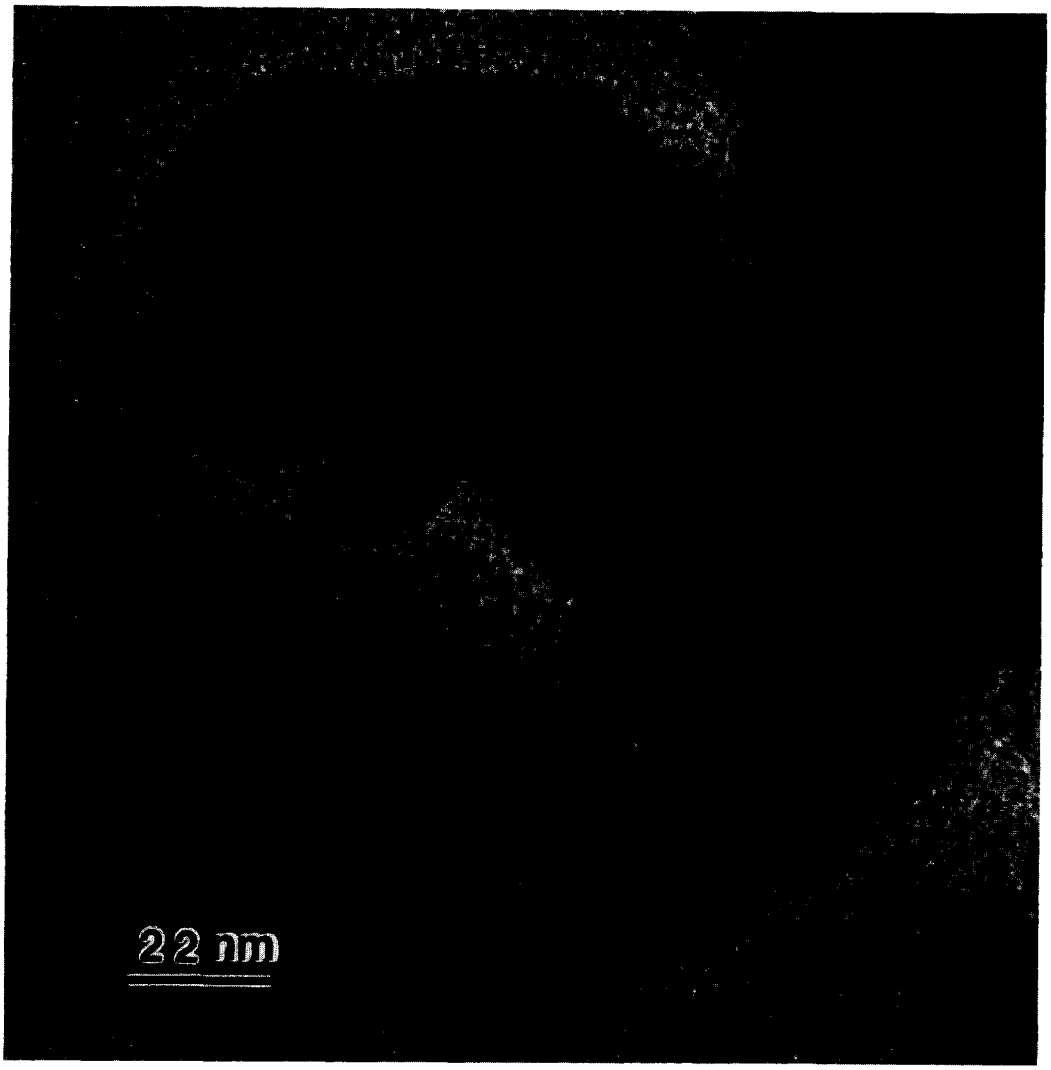

FIG. 13. A bright-field micrograph of an 80-nm cobalt particle. Distance between the faults is observed to be about 3 nm.

particles imaged in Figs. 11 and 12. Stacking faults in a large cobalt particle of about 80 nm in diameter can be clearly seen in a bright field micrograph of CAT-171A (Fig. 13). Two faulted regions of different orientations connected at an interface are shown in Fig. 14. Another interface can also be seen between a smaller particle and a larger one in Fig. 15. Strains associated with such interfaces may give rise to additional catalytic activity. The faults in these TEM micrographs appear to be about 3 nm apart. The average particle size measured from the micrographs of CAT-171A and CAT-65 was found to be 36 nm. The diffracting particle sizes measured by X-ray line broadening were about 15 nm. The difference between the two sizes could be accounted for by particles, on the average, containing a single interface.

The presence of 30% fcc phase could be due to the heavy faulting or it is possible

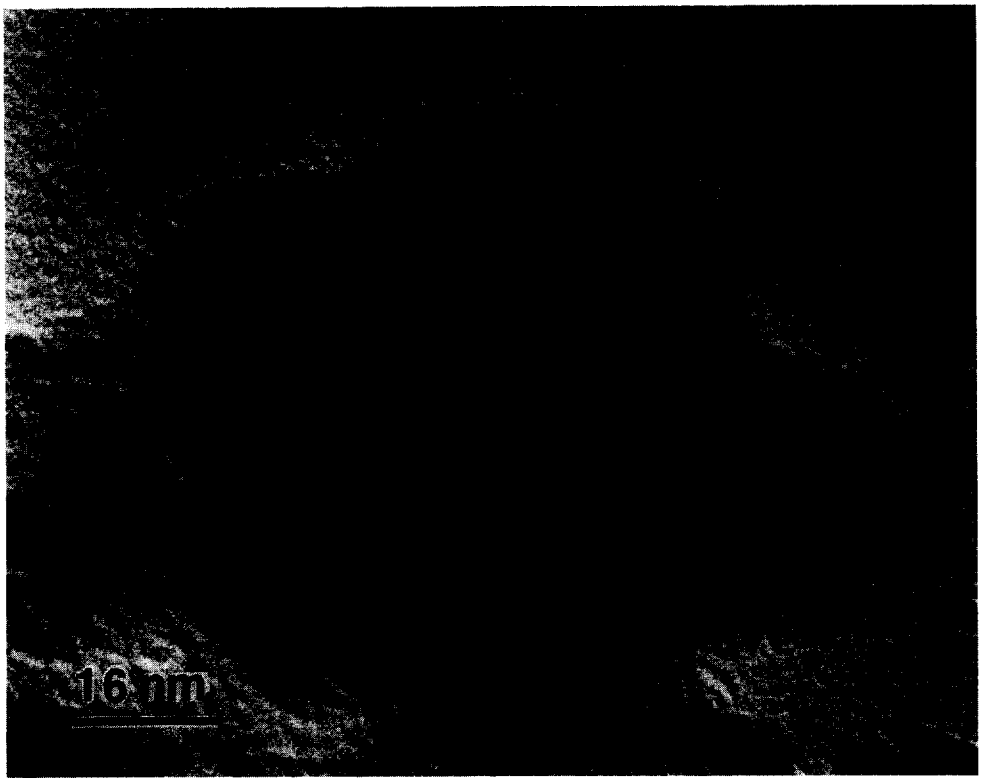

FIG. 14. Fringes in a cobalt particle oriented in different directions, connected at an interface. Strains associated with such interfaces may offer active sites.

that some particles are fcc while others are faulted hcp, or one single particle may consist of both phases. The formation of products of high molecular weight by cobalt particles appears to be related to the existence of faults. The presence of finely dispersed CoO particles is also believed to contribute additional activity. The overall selectivity and activity appear to be controlled by the presence of faulted metallic cobalt and the dispersed form of its oxide.

CONCLUSIONS

It has been confirmed that the method of preparation of silica-supported cobalt catalysts has a significant effect on the phases formed after reduction treatment. CoO phase is completely reduced to metallic cobalt in the catalysts prepared by the physical admixture technique, whereas the aqueous nitrate impregnation method leaves a small amount of unreduced CoO phase. The carbonyl vapor impregnation method yields very fine metallic particles after reduction treatment. The physically admixed catalysts yield a mixture of fcc and hcp phases. Fault densities in silica-supported cobalt catalysts are twice as high as in ZSM-5-supported ones, and this high degree of faulting may be generating a greater number of active sites. One out of every six hcp planes is faulted and the particle size distribution functions of hcp cobalt are mostly bimodal in nature.

ACKNOWLEDGMENTS

The research was sponsored by the Division of Materials Science, U.S. Department of Energy under Contract DE-FG05-85ER45186 at the University of Kentucky, and by the SHaRE program at Oak Ridge

FIG. 15. An interface between a smaller cobalt particle and a larger one.

National Laboratory under Contract DE-AC05-760R00033 with Oak Ridge Associated Universities. Fruitful discussions with Drs. V. U. S. Rao and R. J. Gormley and their help in the preparation of the catalysts are gratefully acknowledged.

REFERENCES

1. Fischer, F., and Tropsch, H., *Brennst. Chem.* **7,** 97 (1926).
2. Fischer, F., *Brennst. Chem.* **24,** 489 (1930).
3. Dhere, A. G., and De Angelis, R. J., *J. Catal.* **92,** 145 (1985).
4. Meisel, S. L., McCullough, J. P., Lechthaler, C. H., and Weisz, P. B., *Chem. Tech.* **6,** 86 (1976).
5. Chang, C. D., and Silvestri, A. J., *J. Catal.* **47,** 247 (1977).
6. Gormley, R. J., Rao, V. U. S., Fauth, D. J., Sprecher, R. F., Pennline, H. W., Youngblood, A. J., and Schehl, R. R., paper presented at the 7th North American Meeting of Catal. Soc., Boston, 1981.
7. Rao, V. U. S., Gormley, R. J., Shamsi, A., Petrick, T. R., Stencel, J. M., Schehl, R. R., and Chi, R. D. H., *J. Mol. Catal.* **29,** 271 (1985).
8. Stencel, J. R., Rao, V. U. S., Diehl, J. R., Rhee, K. H., Dhere, A. G., and De Angelis, R. J., *J. Catal.* **84,** 109 (1983).
9. Denny, P. J., and Whan, D. A., *Catalysis* **2,** 46 (1978).
10. Storch, H. H., Golumbic, N., and Anderson, R. B., "The Fischer–Tropsch and Related Syntheses." Wiley, New York, 1951.
11. Private communication with Rao, V. U. S., and Gormley, R. J.
12. Shamsi, R. J., *et al., INEC Prod. Res. Dev.* **23,** 513 (1984).
13. Ganesan, P., Kuo, H. K., Saavedra, A., and De Angelis, R. J., *J. Catal.* **52,** 310 (1978).
14. Warren, B. E., "X-ray Diffraction," p. 298. Addison–Wesley, Reading, MA, 1968.
15. Rao, V. U. S., *Phys. Scr.* **T4,** 71 (1983).
16. Dhere, A. G., "Structural Characterization of Co/ZSM-5 Catalysts," Ph.D thesis. Univ. of Kentucky, Lexington, 1982.
17. Dhere, A. G., De Angelis, R. J., Reucroft, P. J., and Bentley, J., *J. Mol. Catal.* **20,** 301 (1983).
18. Amariglio, A., Eddouasse, and Amariglio, H., *Surf. Sci.* **162,** 375 (1985).